ORIGINAL ARTICLE

Modelling and analysis of abrasive water jet cutting front profile

Shu Wang[1] · Fengling Yang[1] · Dong Hu[1] · Chuanlin Tang[1] · Peng Lin[1]

Abstract

Abrasive water jet (AWJ) is an advanced manufacturing tool for processing difficult-to-cut materials. However, the further application of AWJ is limited by its achievable machining accuracy. Different from traditional processing methods, the AWJ is a soft knife that will be deformed during processing, so its machining accuracy depends on the cutting front. In this paper, the influence of processing parameters on the cutting front of AWJ is studied in detail. The results show that the nozzle traverse speed has a significant influence on the cutting front profile, while the influence of abrasive flow rate and water pressure on the cutting front profile is not obvious. Based on this, the cutting front profile model is built through theoretical and experimental analysis. With this model, it becomes feasible and practical to predict the cutting front curve based on cutting conditions.

Keywords Abrasive water jet · Cutting front · Modelling · Regression analysis

1 Introduction

When water is pressurized to a high pressure and discharged from a small orifice, the velocity of the water stream can reach as high as 800 m/s. Impingement of such a water stream causes damage to materials such as rocks, plastics, woods, or even some metals by shearing, cracking, and delamination. The abrasive water jet (AWJ) is formed by adding abrasive particles into the high-velocity water stream, which can significantly improve the cutting ability. Compared with traditional machining technologies, the AWJ technology has the advantages of thermal distortion free, high machining versatility, small machining force, and high flexibility [1]. After decades of development, it has been widely used in various industries such as aerospace, defense, automotive, fabrication, and hazardous environment.

Unlike traditional processing methods, the AWJ is a soft knife, which deflects opposite to the direction of the motion during processing. In other words, the exit of the jet from the material lags behind the point at the top of the material where the jet enters. The jet-material interface is called the cutting front (as shown in Fig. 1). As a result, the machining accuracy

of the AWJ depends on the cutting front [2]. Therefore, it is very important to understand the cutting front of the AWJ. The behavior of the cutting front is a major factor that affects the AWJ cutting process [3].

Many researchers have studied the cutting front of AWJ and achieved fruitful research results. Hashish used a high-speed camera to record the process of AWJ cutting transparent materials, and analyzed the formation mechanism of the cutting front curve [4]. By analyzing the cutting front profile, Matsui et al. found that the cutting front curve of AWJ can be represented by the arc, and there is a relationship between the arc radius and the nozzle traverse speed [5]. Zeng et al. researched the stripe traces on the cutting surface, and pointed out that these stripes can be described by parabolas [6]. Kitamura et al. pointed out that the jet lag is linearly related to the nozzle traverse speed, and the slope will increase with the workpiece thickness [7]. Hashish confirmed this rule through experiments [8]. Henning et al. pointed out that in the AWJ cutting process, the energy of the abrasive particles is attenuated, which will change the original curvature of the cutting front curve [9]. Gostimirovic et al. researched the influence of the nozzle traverse speed and the abrasive mass flow rate on the cutting front curve, and optimized the cutting parameters to improve AWJ machining accuracy [10]. Akkurt pointed out that the energy dissipation phenomena in the AWJ cutting process caused the jet-material interface to deviate from the ideal geometric shape, thereby forming a real cutting front morphology. In addition, the cutting front morphology can be expressed by a second-order parabolic formula [11].

✉ Fengling Yang
  yfl_cqu@163.com

1 School of Energy and Electromechanical Engineering, Hunan University of Humanities, Science and Technology, Loudi, China
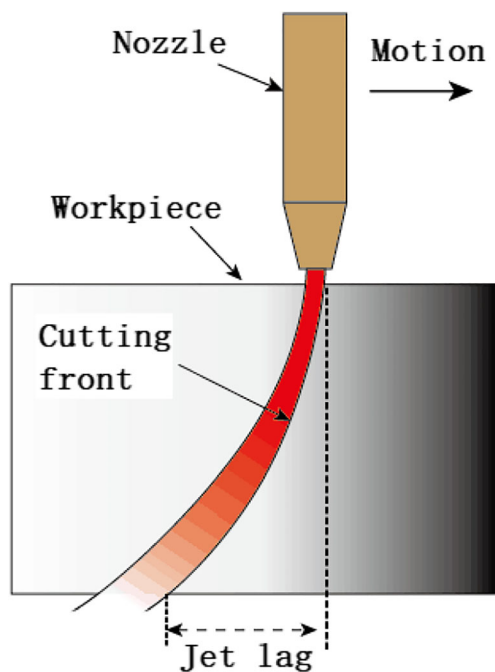
Fig. 1 Cutting front

By studying the cutting front morphology under different processing parameters, Wu et al. also confirmed this phenomenon [12]. In addition, Chen et al. studied the material removal mechanism from the perspective of abrasive jet surface polishing, and expanded the application fields of AWJ [13].

The above research enriched the theoretical system of AWJ processing, but it still cannot meet the requirements of higher-precision processing. In order to improve the processing accuracy of AWJ, it is very important to accurately predict the cutting front profile under the selected processing parameters. Therefore, the relationship between machining parameters and cutting front profile was studied in this paper. On this basis, the model of cutting front profile was established and verified.

2 Experimental study

The cutting front profile changes with the cutting parameters. In order to explore how cutting parameters affect the cutting front, a series of experiments has been carried out on OMAX 2626XP JetMachining Center (as shown in Fig. 2). The parameters such as orifice diameter and abrasive size are not considered in this paper since they are usually unchanged. The workpiece material selected in this paper is aluminum alloy 6061T, which has been widely used in industrial fields. The information of other parameters is shown in Table 1. The cutting quality indicates the moving speed of the nozzle. The lower the cutting quality, the faster the nozzle moving speed and the rougher the cutting surface [14]. Q3–Q10 are called the numbers of the cutting quality, which represent different

Fig. 2 OMAX 2626XP JetMachining Center

levels of the nozzle moving speed. In order to meet the requirements of precision machining, Q3 was chosen for the lowest cutting quality. The specific value of the nozzle moving speed can be obtained through Zeng's model [15]:

$$u = \left(\frac{N_m P_w^{1.25} \dot{m}_w^{0.687} \dot{m}^{0.343}}{C_s q H D^{0.618}} \right)^{1.15} \quad (1)$$

where u is nozzle traverse speed (mm/s), N_m is the machinability number of target material, P_w is the water pressure (MPa), $\dot{m}_w$ is the water flow rate (lpm), $\dot{m}$ is the abrasive flow rate (g/s), C_s is the scale factor, q is the cutting quality, H is the target material thickness (mm), and D is the mixing tube diameter (mm).

After the parameters are determined, the workpiece for cutting is prepared. The length of the workpiece is 50 mm and the width is 20 mm. The AWJ is used to cut a straight line in the middle of each workpiece. In order to obtain accurate data of cutting front, the abrasive feed hose must be removed under a

Table 1 Experimental parameters list

Parameters	Specifications
Target material thickness (mm)	10, 25, 50
Cutting quality	Q3, Q5, Q10
Water pressure (MPa)	245, 315, 385
Abrasive flow rate (kg/min)	0.25, 0.35, 0.45
Standoff distance (mm)	1.5
Abrasive size (mesh)	100
Abrasive type	Garnet
Mixing tube diameter (mm)	0.89
Orifice diameter (mm)	0.33
Target material	Al-6061T

stable cutting speed. The real AWJ cutting front profile obtained by the experiment is shown in Fig. 3. Then, the cutting front can be measured using a digital dial indicator with a fixed hard needle (as shown in Fig. 4). Finally, the accurate cutting front data can be obtained by moving the digital dial indicator along the cutting depth direction.

3 Results and discussions

3.1 Influence of abrasive flow rate on the cutting front profile

As shown in Fig. 5, the influence of abrasive flow rate on the cutting front profile is not obvious. The cutting front curves under different abrasive flow rates are similar, and they are almost parallel or even coincide.

3.2 Influence of water pressure on the cutting front profile

As shown in Fig. 6, the influence of water pressure on the cutting front profile is also not obvious. The cutting front curves under different water pressure conditions are relatively similar, and they are almost parallel or even coincide.

3.3 Influence of nozzle traverse speed on the cutting front profile

Compared with the abrasive flow rate and water pressure, the nozzle traverse speed has a great influence on the cutting front profile, as shown in Fig. 7. The cutting front curves under different nozzle traverse speeds are quite different. When other parameters are fixed, the jet lag will increase with the nozzle traverse speed.
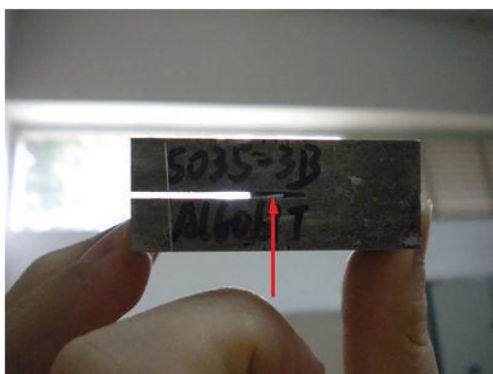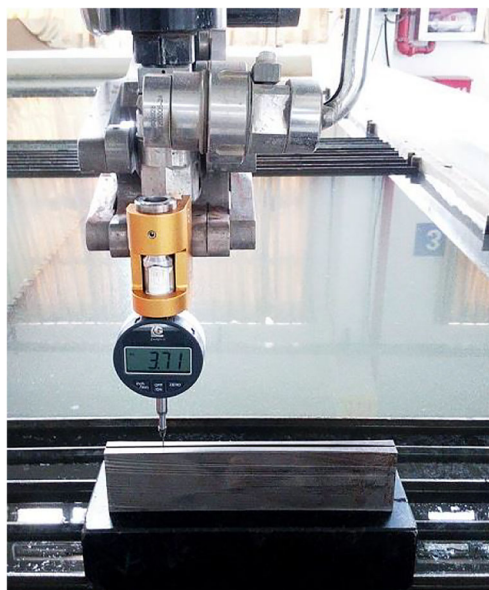

Fig. 3 Real AWJ cutting front profile

Fig. 4 Cutting front data measurement

4 Predictive model for the cutting front profile

4.1 Model development

According to experimental analysis, the cutting front curves are nearly parabolic. Curve-fitting the data with parabolas yields the correlation coefficients between 0.990 and 0.999. Therefore, the cutting front profile can be characterized in terms of a simple functional expression as:

$$J(h) = b_1 h^2 + b_2 h \qquad (2)$$

where b_1 and b_2 are regression coefficients, and h is the cutting depth.

For a group of preset AWJ cutting parameters, the cutting front curves are parallel [16]. Therefore, a continuous cutting process can be modeled as a parabola moving with a constant speed of v, as shown in Fig. 8.

As shown in Fig. 9, the material removal width of the jet on the upper surface of the material is D; usually D can be equivalent to the diameter of the mixing nozzle. The material removal width will decrease as the cutting depth increases, and its changing trend is the same as the attenuation trend of the jet energy along the cutting depth. The cutting front curve is a direct characterization of the jet energy changes along the cutting depth. The diameter of the AWJ gradually decreases along the cutting front curve. The shaded part in Fig. 9 shows the material removal on the upper surface of the material in time t. As the cutting depth increases, the width of the shadow will gradually decrease from D, but the removal speed in the horizontal direction is still maintained at the speed of v. That

Fig. 5 **a** Abrasive flow rate affects cutting front profile (thickness 10mm, water pressure 315MPa, cutting quality 3). **b** Abrasive flow rate affects cutting front profile (thickness 25mm, water pressure 315MPa, cutting quality 3)

Thickness 10mm, water pressure 315MPa, cutting quality 3

(a)

Thickness 25mm, water pressure 315MPa, cutting quality 3
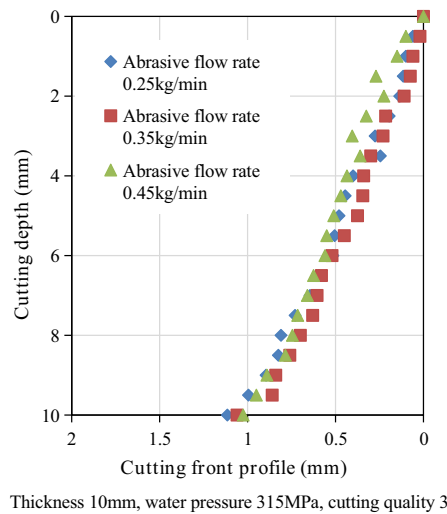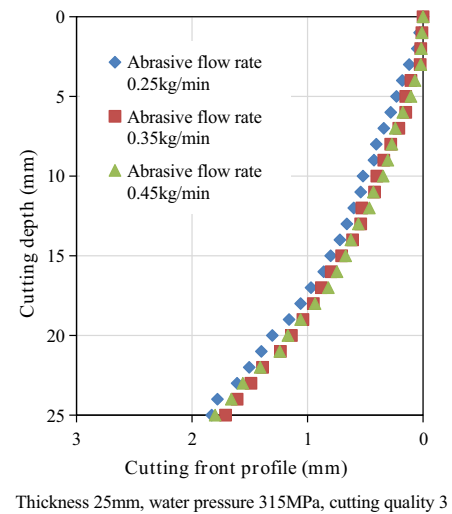
(b)

is, the length of the shaded part remains unchanged. The AWJ is gradually deflected with the cutting front curve. It can be considered that at any point on the cutting front curve, there is a trigonometric function relationship between the volume removal of material d_x in the horizontal direction, the volume removal of material d_s in the tangential direction, and the volume removal of material d_j in the normal direction. The angle between the horizontal direction and the normal direction at this point is θ, as shown in Fig. 9.

The jet maintains a constant material removal speed in the horizontal direction, so the material removal volume per unit time in the horizontal direction at any point on the cutting

front curve is the same as the material removal volume on the upper surface of the workpiece. That is, $d_x = D$, then:

$$d_j = D \cos \theta \qquad (3)$$

The continuous cutting process can be modeled as a parabola moving with a constant speed of v, so the material removal rate in the horizontal direction can be expressed as:

$$\dot{M} = v \qquad (4)$$

Total volume of material removed per unit time can be obtained as:

Fig. 6 **a** Water pressure affects cutting front profile (thickness 25mm, cutting quality 10, abrasive flow rate 0.25kg/min). **b** Water pressure affects cutting front profile (thickness 50mm, cutting quality 5, abrasive flow rate 0.35kg/min)


Thickness 25mm, cutting quality 10, abrasive flow rate 0.25kg/min

(a)

Thickness 50mm, cutting quality 5, abrasive flow rate 0.35kg/min
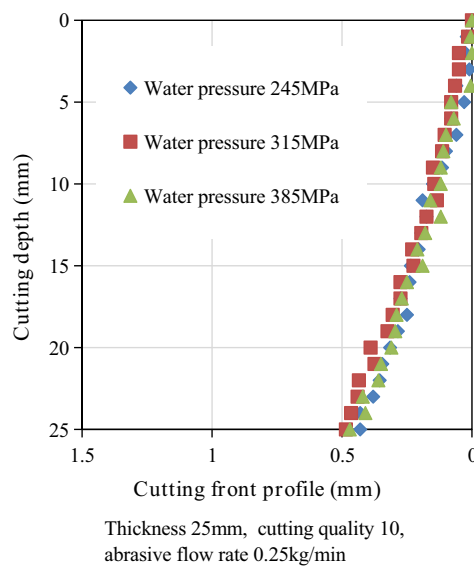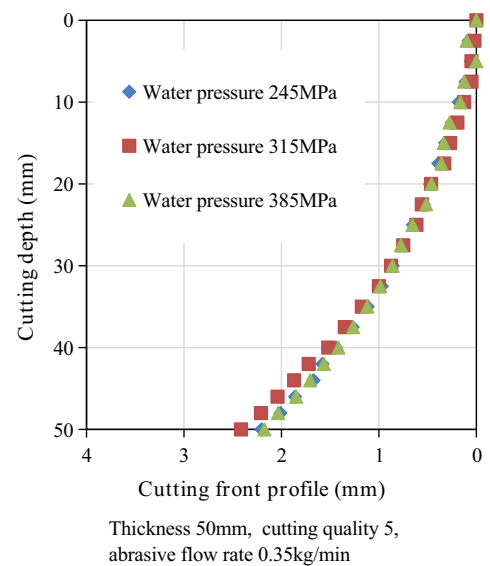
(b)

Fig. 7 a Nozzle traverse speed affects cutting front profile (thickness 10mm, water pressure 385MPa, abrasive flow rate 0.35kg/min). **b** Nozzle traverse speed affects cutting front profile (thickness 50mm, water pressure 245MPa, abrasive flow rate 0.45kg/min)

Thickness 10mm, water pressure 385MPa, abrasive flow rate 0.35kg/min

(a)

Thickness 50mm, water pressure 245MPa, abrasive flow rate 0.45kg/min

(b)
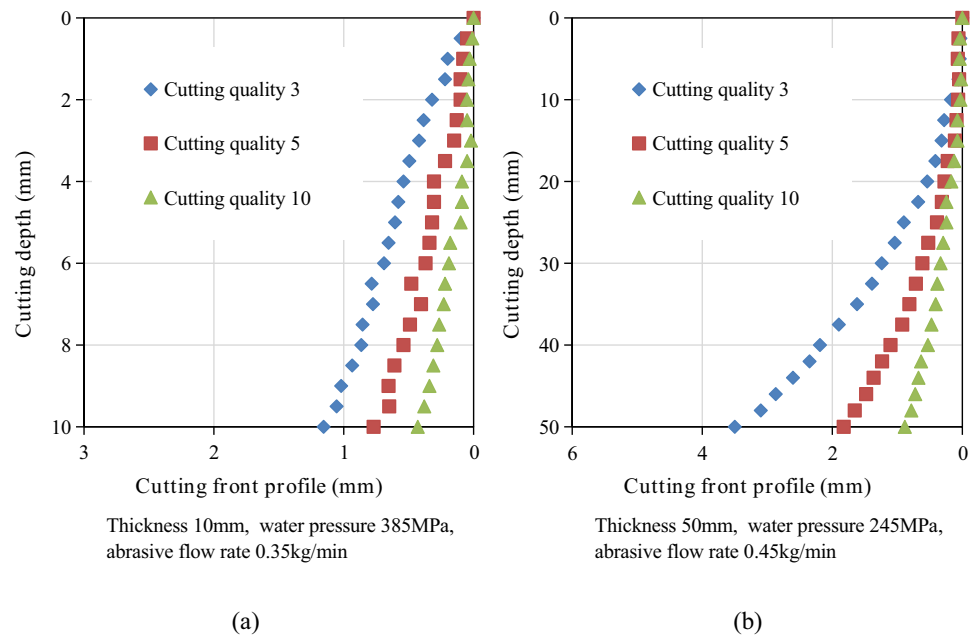
$$Q = \int \dot{M} d_j d_s \tag{5}$$

The AWJ cutting process can be regarded as the cumulative effect of the removal of material by a single abrasive particle, so the total volume of material removed by the jet per unit time can be expressed as:

$$Q = \frac{\dot{m}}{m}\left(\frac{1}{S}\int \cos\theta \, d_s\right)V \tag{6}$$

where m is the average mass of a single abrasive, $\dot{m}$ is the abrasive flow rate, S is the cutting front curve length, and V is the material removal volume of a single abrasive. According to Zeng's research [16], V can be expressed as:

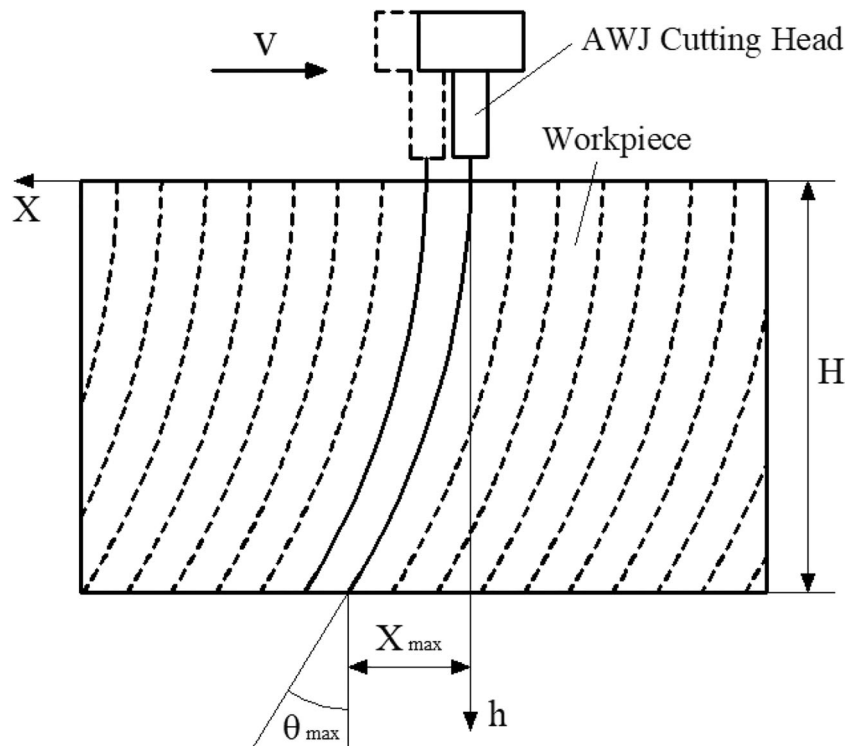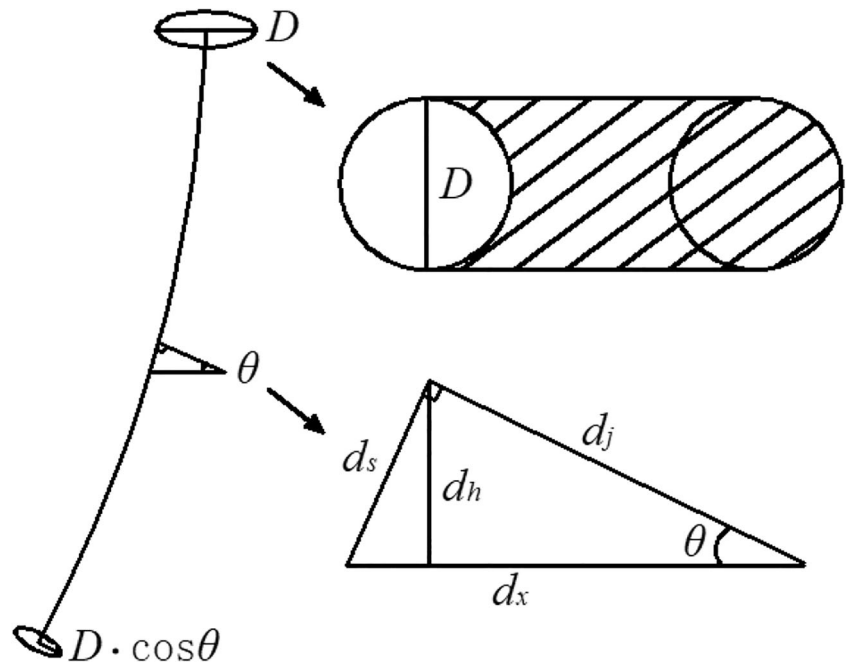**Fig. 8** Model of theoretical processes in a continuous AWJ cutting

Fig. 9 Relationships among volume removal rates

$$V = \left(\frac{\eta C_v C_y}{1+R}\right)^2 \frac{C\dot{m}P}{\rho_w}\left(\frac{2f_w\beta a\sigma_f\alpha^2}{3\gamma E}+\frac{\alpha}{\sigma_f}\right) \quad (7)$$

where η is the momentum transfer coefficient, C_v is the efficiency coefficient of the water nozzle, C_y is the compression coefficient, R is the ratio of abrasive flow rate to water mass flow rate, C is the impact efficiency coefficient, $\dot{m}$ is the abrasive flow rate, ρ_w is the density of water, f_w is the energy

required to form a crack, β is the constant coefficient of the material, a is the grain size of the material, σ_f is the yield stress of the material, γ is the energy required to break the material per unit area, E is the elastic modulus of the material, and α is the impact angle.

Combining Eqs. (2), (5), (6), and (7), the following formula can be obtained:

$$\frac{1}{2b_1}\left[\frac{2b_1h+b_2}{2}\sqrt{(2b_1h+b_2)^2+1}+\frac{1}{2}\ln\left(2b_1h+b+\sqrt{(2b_1h+b_2)^2+1}\right)\right]_0^H$$
$$= \left(\frac{\eta C_v C_y}{1+R}\right)^2\frac{C\dot{m}P}{vD\rho_w}\left(\frac{2f_w\beta a\sigma_f\alpha^2}{3\gamma E}+\frac{\alpha}{\sigma_f}\right) \quad (8)$$

Let:

$$g(h) = \frac{2b_1h+b_2}{2}\sqrt{(2b_1h+b_2)^2+1}+\frac{1}{2}\ln\left(2b_1h+b_2+\sqrt{(2b_1h+b_2)^2+1}\right) \quad (9)$$

Then, Eq. (8) can be simplified to:

$$\frac{g(H)-g(0)}{2b_1} = \left(\frac{\eta C_v C_y}{1+R}\right)^2\frac{C\dot{m}P}{vD\rho_w}\left(\frac{2f_w\beta a\sigma_f\alpha^2}{3\gamma E}+\frac{\alpha}{\sigma_f}\right) \quad (10)$$

Since b_1 is a constant, Eq. (10) can be re-written as follows:

$$g(H)-g(0) = \left(\frac{\eta C_v C_y}{1+R}\right)^2\frac{C_1\dot{m}P}{vD\rho_w}\left(\frac{2f_w\beta a\sigma_f\alpha^2}{3\gamma E}+\frac{\alpha}{\sigma_f}\right) \quad (11)$$

When other parameters remain unchanged, the cutting front curves generated by AWJ cutting materials of different thicknesses are almost the same [17]. And the continuous cutting process can be modeled as a parabola moving with a constant speed. Therefore, Eq. (11) is valid at any cutting depth. The following formula can be obtained:

$$g(h)-g(0) = \left(\frac{\eta C_v C_y}{1+R}\right)^2\frac{C_1\dot{m}P}{vD\rho_w}\left(\frac{2f_w\beta a\sigma_f\alpha^2}{3\gamma E}+\frac{\alpha}{\sigma_f}\right) \quad (12)$$
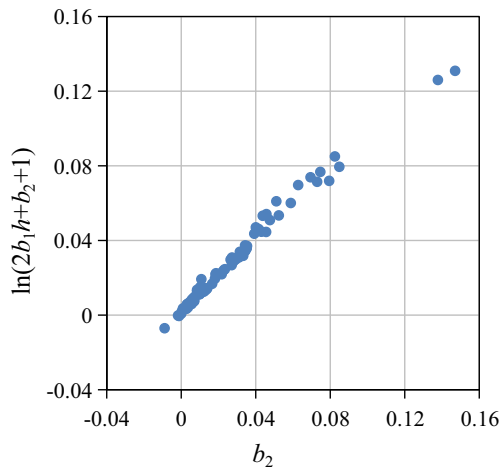
Fig. 10 Relation of b_2 vs. $\ln(2b_1h+b_2+1)$

In the above formula, $g(0)$ is a certain value, so it can also be treated as a constant term. Eq. (12) can be re-written as follows:

$$g(h) = \left(\frac{\eta C_v C_y}{1+R}\right)^2 \frac{C_1 \dot{m} P}{v D \rho_w} \left(\frac{2f_w \beta a \sigma_f \alpha^2}{3\gamma E} + \frac{\alpha}{\sigma_f}\right) + C_2 \quad (13)$$

Curve-fitting the cutting front data in this paper with Eq. (2) yields:

$$(2b_1h + b_2)^2 \ll 1, \qquad b_2^2 \ll 1 \quad (14)$$

Then, Eq. (9) can be approximately simplified to:

$$g(h) = \frac{1}{2}[2b_1h + b_2 + \ln(2b_1h + b_2 + 1)] \quad (15)$$

Based on the analysis of experimental data, it is found that $\ln(2b_1h+b_2+1)$ and b_2 are almost equal, as shown in Fig. 10. Therefore, b_2 can be used in place of $\ln(2b_1h+b_2+1)$, so Eq. (15) can be transformed into:

$$g(h) = b_1h + b_2 \quad (16)$$

Combining Eqs. (2), (13), and (16), the following formula can be obtained:

$$\frac{J(h)}{h} = \left(\frac{\eta C_v C_y}{1+R}\right)^2 \frac{C_1 \dot{m} P}{v D \rho_w} \left(\frac{2f_w \beta a \sigma_f \alpha^2}{3\gamma E} + \frac{\alpha}{\sigma_f}\right) + C_2 \quad (17)$$

Analyzing the Eq. (17), some parameters are fixed in this paper, and they can be treated as constants. So Eq. (17) can be simplified to:

$$\frac{J(h)}{h} = \frac{C_3 \dot{m} P}{v} \quad (18)$$

Then, the following regression coefficient model can be established:

$$J(h) = C_0 P^{n_1} \dot{m}^{n_2} h^{n_3} v^{n_4} \quad (19)$$

where $J(h)$ is the change value of the cutting front with the cutting depth (m), P is the water pressure (Pa), $\dot{m}$ is the abrasive flow rate (kg/s), h is the cutting depth (m), v is the nozzle traverse speed (m/s), and $n_1–n_4$ are the regression coefficients.

So, by using regression analysis method, the cutting front profile model can be gotten as following:

$$J(h) = \frac{1219462.805 h^{1.6226} v^{0.7663}}{P^{0.6027} \dot{m}^{0.497}} \quad (20)$$

The fitting parameters are listed as follows:

n_1: -0.602711557
n_2: -0.496962206
n_3: 1.622551986
n_4: 0.766323612
C_0: 1219462.805
RMSE: 0.000137418384744087
SSE: $3.77298573064167E-5$
R: 0.981012155096286
R^2: 0.96238484844666
DC: 0.962227531971829
Chi-square: 0.0326148513801527
F-Statistic: 51067.7234617965

Table 2 Verification experiment parameters

Nozzle traverse speed (mm/min)	Target material thickness (mm)	Water pressure (MPa)	Abrasive flow rate (kg/min)
132.73	10	245	0.202
86.46	10	385	0.427
54.75	25	245	0.315
31.79	25	245	0.406
16.31	50	315	0.227
23.14	50	315	0.421

4.2 Model validation

A series of verification tests were carried out to verify the accuracy of the model. The test parameters are shown in Table 2. Except for the parameters listed in Table 2, the other parameters are exactly the same as the previous ones. The Pearson correlation coefficients between the test values and the calculated values are 0.9954, 0.9711, 0.9978, 0.9952, 0.9973, and 0.9986. Parts of the comparisons between the test values and the calculated values are shown in Fig. 11. The results show that the model established in this paper can be used to predict the cutting front profile according to the given processing parameters.

Fig. 11 a Comparison of predicted and testing curves (thickness 10mm, nozzle traverse speed 132.73mm/min, abrasive flow rate 0.202kg/min, water pressure 245MPa). **b** Comparison of predicted and testing curves (thickness 10mm, nozzle traverse speed 86.46mm/min, abrasive flow rate 0.427kg/min, water pressure 385MPa). **c** Comparison of predicted and testing curves (thickness 25mm, nozzle traverse speed 54.75mm/min, abrasive flow rate 0.315kg/min, water pressure 245MPa). **d** Comparison of predicted and testing curves (thickness 50mm, nozzle traverse speed 16.31mm/min, abrasive flow rate 0.227kg/min, water pressure 315MPa)

Thickness 10mm, nozzle traverse speed 132.73mm/min, abrasive flow rate 0.202kg/min, water pressure 245MPa

(a)

Thickness 10mm, nozzle traverse speed 86.46mm/min, abrasive flow rate 0.427kg/min, water pressure 385MPa

(b)

Thickness 25mm, nozzle traverse speed 54.75mm/min, abrasive flow rate 0.315kg/min, water pressure 245MPa

(c)

Thickness 50mm, nozzle traverse speed 16.31mm/min, abrasive flow rate 0.227kg/min, water pressure 315MPa

(d)
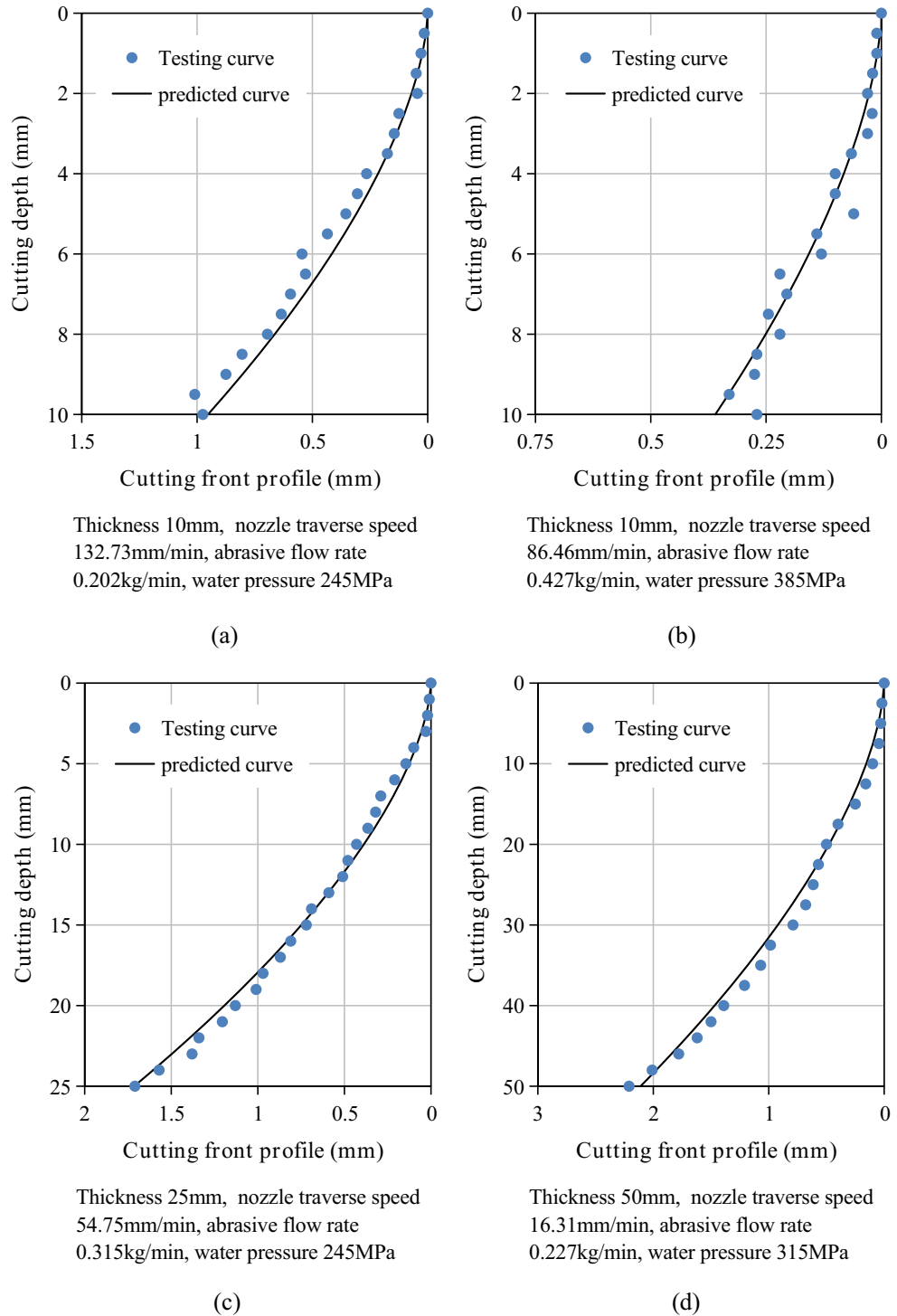
5 Conclusions

The influence of abrasive flow rate on the cutting front profile is not obvious. The cutting front curves under different abrasive flow rates are similar, and they are almost parallel or even coincide. The influence of water pressure on the cutting front profile is similar to that of the abrasive flow rate. The nozzle traverse speed has a great influence on the cutting front profile. The cutting front curves under different nozzle traverse speeds are quite different. When other parameters are fixed, the jet lag will increase with the nozzle traverse speed.

The cutting front curve can be described by a parabola. And for a group of preset AWJ cutting parameters, the cutting front curves are parallel. Therefore, a continuous cutting process can be modeled as a parabola moving with a constant speed. Based on this, Zeng's erosion theory is introduced, and the relationship between the cutting front curve and the cutting depth is established through theoretical and experimental analysis. Then, the cutting front profile model is built by using regression analysis method, which is beneficial to improve the machining accuracy of AWJ.

Author contribution Shu Wang: conceptualization, experiments, and writing; Fengling Yang: conceptualization, funding acquisition, and project supervision; Dong Hu: data analysis and writing; Chuanlin Tang: supervision, investigation, and data curation; Peng Lin: experiments.

Data availability All data is published with the paper.

Declarations

Ethical approval   This work does not contain any ethical issues or personal information.

Consent to participate   No human or animal was involved in this work; thus, no consent was required.

Consent for publication   All authors have given their permission for publishing this work.

Competing interests   The authors declare no competing interests.

References

1. Chen M, Zhang S, Zeng J, Chen B (2019) Correcting shape error located in cut-in/cut-out region in abrasive water jet cutting process. Int J Adv Manuf Technol 102(5-8):1165–1178

2. Zhang S, Wu Y, Wang S (2015) An exploration of an abrasive water jet cutting front profile. Int J Adv Manuf Technol 80(9-12):1685–1688

3. Henning A, Westkamper E (2006) Analysis of the cutting front in abrasive waterjet cutting. In: Proceedings of the 18th international conference on water jetting. Gdansk, Poland, pp 425–434

4. Hashish M (1988) Visualization of the abrasive waterjet cutting process. Exp Mech 28(2):159–169

5. Matsui S, Matsumura H, Ikemoto Y, Tsujita K, Shimizu H (1990) High precision cutting method for metallic materials by abrasive waterjet. In: Proceedings of the 10th International Symposium. The Netherlands, Amsterdam, pp 263–278

6. Zeng J, Heines R, Kim TJ (1991) Characterization of energy dissipation phenomenon in abrasive waterjet cutting. In: Proceedings of the 6th American waterjet conference. Houston, Texas, USA, pp 163–177

7. Kitamura M, Ishikawa M, Sudo K, Yamaguchi Y, Tujita K (1992) Cutting of steam turbine components using an abrasive water jet. Jet Cutting Technology. Springer Netherlands, pp. 543-554.

8. Hashish M (2007) Benefits of dynamic waterjet angle compensation. In: 2007 American WJTA Conference and Expo, Houston, Texas, USA. pp. 1-H.

9. Henning A, Westkamper E, Schmidt B (2004) Analysis of geometry at abrasive waterjet cutting operation. In: Proceedings of the 17th international conference on water jetting-advances and future needs. Mainz, Germany, pp 465–474

10. Gostimirovic M, Pucovsky V, Sekulic M, Rodicet D, Pejic V (2019) Evolutionary optimization of jet lag in the abrasive water jet machining. Int J Adv Manuf Technol 101:3131–3141

11. Akkurt A (2010) Cut front geometry characterization in cutting applications of brass with abrasive water jet. J Mater Eng Perform 19(4):599–606

12. Wu Y, Zhang S, Wang S, Yang F, Tao H (2015) Method of obtaining accurate jet lag information in abrasive water-jet machining process. Int J Adv Manuf Technol 76(9-12):1827–1835

13. Chen F, Tang Y, Miao X, Yin S (2015) Review on the abrasive jet surface polishing (AJP) technology. Surf Technol 44(11):119–127

14. Zeng J (2007) Determination of machinability and abrasive cutting properties in AWJ cutting. In: 2007 American WJTA Conference and Expo, Houston, Texas, pp. 19-21.

15. Zeng J, Kim TJ, Wallace RJ (1992) Quantitative evaluation of machinability in abrasive water-jet machining. In: Proceedings of the 1992 winter annual meeting of ASME, precision machining: technology and machine development and improvement. Anaheim, PED-58, pp. 169-179.

16. Zeng J (1992) Mechanisms of brittle material erosion associated with high pressure abrasive waterjet processing-a modeling and application study. University of Rhode Island, Dissertation

17. Henning A, Anders S (1998) Cutting-edge quality improvements through geometrical modeling. In: Proceedings of the 14th International Conference on Jetting Technology. Brugge, Belgium, pp 321–328

Publisher's note Springer Nature remains neutral with regard to jurisdictional claims in published maps and institutional affiliations.